Target Tracking on Sensing Surface with Electrical Impedance Tomography

Timo Huuhtanen
Department of Computer Science
Aalto University
Espoo, Finland
timo.huuhtanen (at) aalto.fi

Antti Lankinen
Department of Bioengineering
Imperial College
London, United Kingdom
antti.lankinen15 (at) imperial.ac.uk

Alexander Jung
Department of Computer Science
Aalto University
Espoo, Finland
alexander.jung (at) aalto.fi

***Abstract*—An emerging class of applications uses sensing surfaces, where sensor data is collected from a 2-dimensional surface covering a large spatial area. Sensing surface applications range from observing human activity to detecting failures of construction materials. Electrical impedance tomography (EIT) is an imaging technology, which has been successfully applied to imaging in several important application domains such as medicine, geophysics, and process industry. EIT is a low-cost technology offering high temporal resolution, which makes it a potential technology sensing surfaces. In this paper, we evaluate the applicability of EIT algorithms for tracking a small moving object on a 2D sensing surface. We compare standard EIT algorithms for this purpose and develop a method which models the movement of a small target on a sensing surface using hidden Markov models (HMM). Existing EIT methods are geared towards high image quality instead of smooth target trajectories, which makes them suboptimal for target tracking. Numerical experiments indicate that our proposed method outperforms existing EIT methods in target tracking accuracy.**

***Index Terms*—Electrical impedance tomography, hidden Markov models, sensing surface**

I. Introduction

An emerging class of sensor applications is sensing surfaces, where sensor data is collected from a 2-dimensional surface covering a large spatial area. These applications aim at detecting interesting events on the surface, capturing the spatial location of the event, and tracking the change of the location in time. Sensing surface applications include observing human activity [1], human-to-machine interface (HMI) [2], sensing skin in robotic applications [3], and detection of failures of construction materials [4]. The target to be tracked in a sensing surface may be e.g. (part of) a human being. Detection is then based on measuring impedance changes caused by some physical phenomenon (e.g. proximity of the target causing a local change in surface impedance). If the target is moving, the problem becomes a target tracking problem combined with a detection/sensing problem. To this end, low-cost measurement technology and efficient detection/tracking algorithms are needed.

Electrical impedance tomography (EIT) can be used for studying the electrical conductivity of a 2-dimensional surface by injecting currents and measuring voltages via electrodes attached to the boundary of the surface. The resulting set of voltage measurements is used to create an image of the conductivity distribution by solving the corresponding inverse problem. EIT is a low-cost method, which has been used successfully in several application areas, such as medical imaging, process industry, and geophysical measurements. EIT's high temporal resolution makes it potential for sensing surface applications, and some work on that has been reported [2], [5].

In this paper, we apply EIT on tracking the location of a moving target on a 2-dimensional conductive surface. The requirements of target tracking differ from those of static imaging applications that aim at the preservation of details, edges, and shapes in the image. When tracking a target on a surface, the location of the target and accurate tracking of its movement are important. Therefore, traditional EIT algorithms are suboptimal for this application as indicated by our simulation results in Section IV.

Detection of the location of a single small-sized target in EIT has been studied in [6]. However, there the targets are static and temporal information is not utilized. [7] describes a case where EIT is used for tracking underwater objects. Temporal EIT methods have been compared in [8]. Reconstructing the image for each time instance independently tends to result in non-smooth trajectories for moving targets. Improved temporal EIT image reconstruction methods have been proposed: [9] proposes the use of Kalman filters, [10] uses extended Kalman filters, and [8] uses the measurement data from several time instances to reconstruct the image for one instance of time. All these methods operate with EIT voltage measurements, where the utilization of detailed target movement information is difficult.

Our approach combines the EIT inverse problem with a model of the target movement (trajectory). The trajectory of a moving target is smooth and the speed is limited (the precise limit depending on the application). The proposed method models the moving target with the hidden Markov model (HMM) and finds the most likely trajectory with the Viterbi algorithm. Kalman filter methods ([10], [9]) are also based on HMMs, but there HMM is used to model the conductivity, and the location of the target is found with postprocessing. In our method, the state of HMM is an index of the mesh directly indicating the location of the target. We compare the performance of our algorithm with state-of-the-

art EIT temporal image reconstruction algorithms on synthetic data. Our method outperforms traditional EIT reconstruction methods in target tracking accuracy.

The remaining part of this paper is organized as follows. In Section II, we describe the EIT measurement setup and the standard nontemporal EIT image reconstruction. In Section III, we formulate the temporal EIT image reconstruction problem and describe the compared methods. The numerical experiments are discussed in Section IV. Section V presents a conclusion and discusses follow-up research directions.

Notation: Boldface lowercase (uppercase) letters denote vectors (matrices). The transpose of a matrix $\mathbf{X}$ is denoted by $\mathbf{X}^T$. We denote the probability of event x by $P(x)$ and the probability density function of random variable X by p_X. For a vector $\mathbf{x} \in \mathbb{R}^n$, $\mathbf{x}_+ = [\max(x_1, 0) \dots \max(x_n, 0)]^T$. Diagonal of a matrix is

$$\text{diag} : \mathbb{R}^{n\times n} \to \mathbb{R}^{n\times n}, \text{diag}(\mathbf{X}) = \begin{bmatrix} \mathbf{X}_{1,1} & & \\ & \ddots & \\ & & \mathbf{X}_{n,n} \end{bmatrix}.$$

II. EIT SETUP

We consider an EIT system with n_e electrodes $e_1 \dots e_{n_e}$ on the boundary of a conductive surface Ω. Using the electrodes, n_e drive current patterns are applied. Voltage differences between adjacent electrodes are measured as illustrated in Fig. 1 (b). The electrodes where currents are applied are excluded from the voltage measurements resulting $n_V = n_e - 4$ voltage measurements $v_k, k \in 1, \dots, n_V$. The voltage measurements from n_e patterns are collected into a vector $\mathbf{v} \in \mathbb{R}^{n_M}$, where $n_M = n_V n_e$.

We consider difference EIT [8] where voltages and conductivities are compared against those obtained for an empty sensing surface. In particular, we use difference measurements $\mathbf{y} = \mathbf{v} - \mathbf{v}_0$ with the reference voltage measurements $\mathbf{v}_0$ measured from an empty sensing surface with conductivity $\boldsymbol{\sigma_0}$. We assume that $\mathbf{v}_0$ is noise-free as it can be averaged from multiple measurements when the surface is known to be empty. We denote the difference data collected at time t with $\mathbf{y}(t)$.

The coupling between currents, voltages, and conductivity at Ω can be derived from Maxwell's equations [11]. If we know the currents I_l implied to the electrodes and assume a conductivity σ in Ω, we can solve the EIT forward problem; i.e. calculate estimates for the electric potential u in Ω. We model the surface as a finite element mesh with n_N triangular elements. Conductivity distribution is approximated as being constant within each element. The electric potential values for each element can then be calculated using the finite element method (FEM). Possible meshes for forward and inverse problems are illustrated in Fig. 2. Typically different meshes are used for forward and inverse problems to avoid *inverse crime* [8]. Typically also the inverse mesh is sparser than the forward mesh.

The EIT inverse problem amounts to recovering $\boldsymbol{\sigma}$ from the measurements $\mathbf{v}$ and can be formalized as

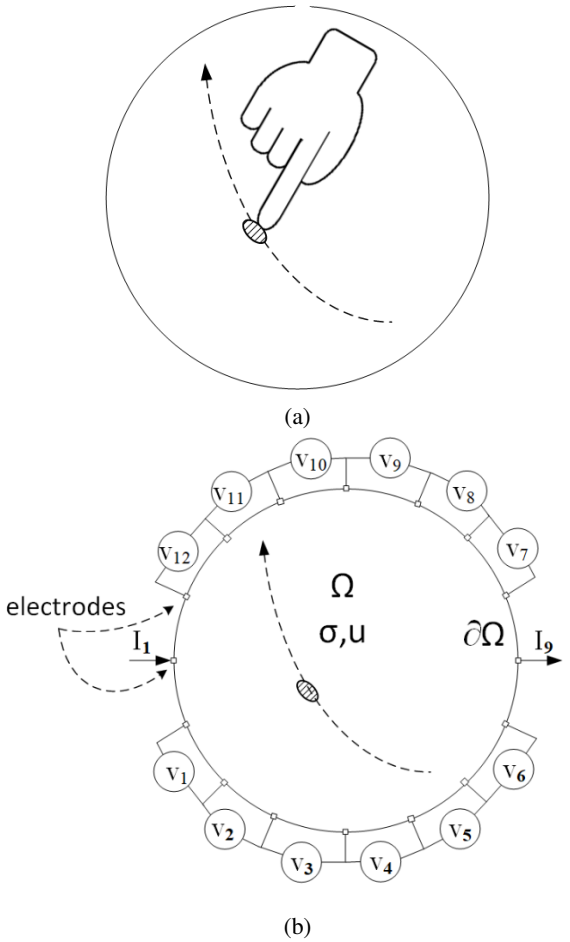

Fig. 1: a) EIT aims at tracking a target (e.g., touch spot of a finger) on a sensing surface. b) EIT measurement setup: electrical current patterns $I^{(l)}$ are applied to electrodes attached to the boundary $\partial\Omega$ and electric potential differences v_k measured between consecutive electrodes.

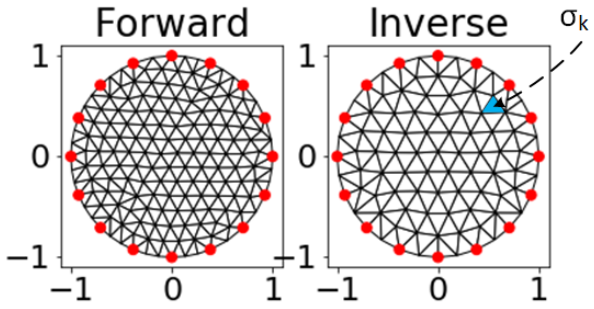

Fig. 2: Finite element meshes used in forward and inverse problems. σ_k indicates the conductivity value - i.e. the solution of the inverse problem for one mesh element.

$$\arg\min_{\boldsymbol{\sigma}} \|\mathbf{v} - \mathbf{u}(\boldsymbol{\sigma})\|_2^2. \quad (1)$$

Here $\mathbf{u}(\boldsymbol{\sigma}) \in \mathbb{R}^{n_M}$ is the concatenation of voltage differences between consecutive electrodes calculated from the model, and $\mathbf{v}$ includes the corresponding measured voltage differences. We use a numeric FEM library [12] to calculate the values of $\mathbf{u}$ as well as the sensitivity matrix or Jacobian $\mathbf{J}$ ($J_{ij} = \frac{\partial u_i}{\partial \sigma_j}$).

We stack the conductivities for each mesh element into the vector $\boldsymbol{\sigma} \in \mathbb{R}^{n_N}$. The values for $\mathbf{u}$ can then be linearized at an estimated reference conductivity $\boldsymbol{\sigma}_0$:

$$\mathbf{u}(\boldsymbol{\sigma}) = \mathbf{u_0} + \mathbf{J}(\boldsymbol{\sigma} - \boldsymbol{\sigma_0}). \quad (2)$$

We denote the differential conductivity $\boldsymbol{\sigma} - \boldsymbol{\sigma}_0$ at time t by $\mathbf{x}(t)$, where each element $x_i(t)$ corresponds to conductivity difference value at one triangular element of the inverse mesh. Inserting (2) into (1) gives

$$\arg\min_{\mathbf{x}\in\mathbb{R}^{n_N}} \|\mathbf{y} - \mathbf{J}\mathbf{x}\|_2^2. \quad (3)$$

This system is typically underdetermined ($n_N > n_M$) and regularization is required. Standard choices for regularization are L_1, L_2 and total variation (TV) regularization [13], [14]. Here we are interested in finding the location of x and do not care about the preservation of shape or size of the target in the reconstructed image of x values. So, we select L_2, which fits well into the detection of the center point location of the target. The regularized version of (1) then becomes

$$\arg\min_{\mathbf{x}} \|\mathbf{y} - \mathbf{J}\mathbf{x}\|_2^2 + \lambda\|\mathbf{R}\mathbf{x}\|_2^2. \quad (4)$$

Here λ is a hyperparameter and $\mathbf{R}$ is a regularization matrix containing some prior information about $\mathbf{x}$. If all the elements of $\mathbf{x}$ are assumed to be statistically independent and have equal means, $\mathbf{R}$ is the identity matrix $\mathbf{I}$. [8] proposes a method, where $\mathbf{R}$ is being scaled with the sensitivity of each element, so that $\mathbf{R} = (\mathrm{diag}(\mathbf{J}^T\mathbf{J}))^p$ for some exponent $p \in [0, 1]$. The choice of p determines whether the noise is pushed to the boundary ($p = 0$) or center ($p = 1$). We use $p = 1/2$ which has been found as a good compromise [8].

The problem now reads

$$\hat{\mathbf{x}} = \arg\min_{\mathbf{x}} \|\mathbf{y} - \mathbf{J}\mathbf{x}\|_2^2 + \lambda\|\mathrm{diag}(\mathbf{J}^T\mathbf{J}))^{0.5}\mathbf{x}\|_2^2, \quad (5)$$

and can be solved in closed form as

$$\hat{\mathbf{x}} = (\mathbf{J}^T\ \mathbf{J} + \lambda\ \mathrm{diag}(\mathbf{J}^T\ \mathbf{J})^{0.5})^{-1}\mathbf{J}^T\mathbf{y} \quad (6)$$

$$= \mathbf{H}\mathbf{y}. \quad (7)$$

III. Methods

We compare three methods for tracking a moving target with EIT:

- Standard nontemporal EIT image reconstruction described in Section II
- The method based on the Kalman filter [9]
- Our novel method based on HMM of the moving target

A. Kalman filter

The temporal EIT method presented in [9] utilizes Kalman filter to model the temporal changes of the conductivity. The Kalman filter can be used to estimate a time-dynamic model for the conductivity as

$$\mathbf{x}(t+1) = \mathbf{A}\mathbf{x}(t) + \mathbf{n}_x(t). \quad (8)$$

The observation process is given by

$$\mathbf{y}(t) = \mathbf{J}\mathbf{x}(t) + \mathbf{n}_y(t). \quad (9)$$

where the conductivity $\mathbf{x}$ is observed via the EIT measurements.

The model parameter $\mathbf{A} \in \mathbb{R}^{n_N \times n_N}$ is the state transition matrix, which defines the dynamic properties of the conductivity, $\sigma(t)$. $\mathbf{n}_x(t) \sim \mathcal{N}(\mathbf{0}, \boldsymbol{\Sigma}_\mathbf{x})$ and $\mathbf{n}_y(t) \sim \mathcal{N}(\mathbf{0}, \boldsymbol{\Sigma}_\mathbf{y})$ are noise in the state transition and observation models, respectively. As in [9], we model them to be white noise processes with covariance matrices $\boldsymbol{\Sigma}_\mathbf{x} = 0.8\mathbf{I}$ and $\boldsymbol{\Sigma}_\mathbf{y} = 0.2\mathbf{I}$.

For $\mathbf{A}$ we use the identity matrix as in [9] and [8]. This choice corresponds to a random walk model for the movements i.e. the target is stationary, movement is driven by the white noise process in (8).

B. Hidden Markov model for EIT

We model the target movement using the following assumptions:

- h1 There is only a single small target (occupying exactly one mesh element) moving on the surface.
- h2 The movement of the target follows a random walk which is slow in comparison to the EIT sampling rate. So, within one instance of time, the target may move to one of the adjacent mesh elements of the inverse solution mesh.
- h3 The target increases the conductivity of the sensing surface. We can assume this without loss of generality since we can replace the definition $\mathbf{x}(t) = \boldsymbol{\sigma} - \boldsymbol{\sigma}_0$ with $\mathbf{x}(t) = \boldsymbol{\sigma}_0 - \boldsymbol{\sigma}$ if the target decreases the conductivity of the sensing surface.

We can model the moving target using a hidden Markov model consisting of random variables $Q(t) \in [M]$ (state) and $Z(t) \in \mathbb{R}^{n_M}$ (observation). Here M denotes the number of elements in the inverse solution mesh. In our context, $Q(t)$ corresponds to the location of the target at time t and $Z(t)$ is the voltage measurement at time t, $\mathbf{y}(t)$. We can solve the most likely sequence of states with the Viterbi algorithm [15]. For T measurements, the parameters of the HMM required for the Viterbi algorithm consist of a transition matrix $\mathbf{P} \in \mathbb{R}^{M\times M}$ and emission matrix $\mathbf{E} \in \mathbb{R}^{M\times T}$ with $\mathbf{P}_{i,j} = P(Q(t+1) = i|Q(t) = j)$ and $\mathbf{E}_{i,j} = P(Z(j)|Q(j) = i)$.

If we assume that the target has equal probabilities to stay in its current location or move to one of its neighboring elements, we can construct the transition probability matrix as follows. Let $\mathbf{S} \in \mathbb{R}^{M\times M}$ be the adjacency matrix of the mesh elements such that $\mathbf{S}_{i,j} = 1$ if elements i, j share an edge or a node and 0 otherwise. Let $\mathbf{D} \in \mathbb{R}^{M\times M}$ be the diagonal degree matrix

such that $\mathbf{D}_{i,i} = \Sigma_{k=1}^{M} \mathbf{S}_{k,i}$. Then the transition matrix is given by

$$\mathbf{P} = (\mathbf{D} + \mathbf{I})^{-1}(\mathbf{S} + \mathbf{I}). \tag{10}$$

For the emission probabilities, we need to compute $P(\mathbf{z}|q)$ for all the states q and voltage measurements $\mathbf{z}$. Using Bayes' theorem, we get

$$P(\mathbf{z}|q) = \frac{P(q\ |\mathbf{z})P(\mathbf{z})}{P(q)}. \tag{11}$$

We argue that the normalized solution for the inverse problem (7)

$$\tilde{\mathbf{x}} = \hat{\mathbf{x}}_+ / \|\hat{\mathbf{x}}_+\|_1 \tag{12}$$

can be used as an estimate for $P(q|\mathbf{z})$. It fulfills the formal requirements of a probability mass function ($\tilde{x}_i \in [0, 1]$ and $\Sigma_i \tilde{x}_i = 1$), and it is the ideal solution of the inverse problem where only one mesh element has nonzero value (due to assumptions h1 and h3).

The quantity $P(\mathbf{z})$ in (11) is the probability of voltage measurement $\mathbf{z}$. The value of the probability density function (pdf) of the distribution at $\mathbf{z}$ gives a relative measure of probability. We modelled the pdf as a Gaussian mixture model learned from the data. $P(q)$ is the probability of state q in the stationary distribution of $\mathbf{P}$ which we can denote as $\boldsymbol{\pi}$.

Let p_Z denote the estimated pdf of Z, $\boldsymbol{\pi}$ the stationary distribution of $\mathbf{P}$, and $\tilde{\mathbf{x}}$ as in (12). Then (11) becomes

$$P(\mathbf{z}|q) = \frac{\tilde{x}_q p_Z(\mathbf{z})}{\pi_q}. \tag{13}$$

Combining (7) and (12) to (13) yields

$$\mathbf{E}_{i,j} = \frac{((\mathbf{H}\mathbf{y}(j))_+)_i p_Z(\mathbf{v}_j)}{\|(\mathbf{H}\mathbf{y}(j))_+\|_1 \pi_i}. \tag{14}$$

With the above formulations, we can compute the most likely sequence of states, $\{q_1, ..., q_T\}$, with the Viterbi algorithm (Algorithm 1). The prior state probability distribution used is the stationary distribution if no prior information is available. When applying the algorithm for real-time tracking, the prior state can be obtained from the last state of the previous sequence.

Algorithm 1 Viterbi($\pi, \mathbf{P}, \mathbf{E}$)

for $i = 1, ..., M$ **do**
  $T_{prob}[i, 1] \leftarrow \pi_i E_{i,1}$
  $T_{state}[i, 1] \leftarrow 0$
end for
for $j = 2, ..., T$ **do**
  for $i = 1, ..., M$ **do**
    $T_{prob}[i, j] \leftarrow \max_k (T_{prob}[i, j-1] P_{k,j} E_{i,j})$
    $T_{state}[i, j] \leftarrow \arg\max_k (T_{prob}[i, j-1] P_{k,j} E_{i,j})$
  end for
end for
$q_T \leftarrow \arg\max_k (T_{prob}[k, T])$
for $j = T, T-1, ..., 2$ **do**
  $q_{j-1} \leftarrow T_{state}[q_j, j]$
end for
return $\{q_1, ..., q_T\}$

IV. Numerical experiments

We compared the performance of the three methods for tracking a single small target. In the first method, we used (7) for each frame to calculate the conductivity and assume the target to be located in the element with the highest conductivity value. In the second method, we calculated the conductivity estimate from the Kalman filter (8), (9). In the third method, we used the transition matrix (10) and emission matrix (14) for the Viterbi algorithm and selected the center of the element where the target is at time t in the Viterbi path as location estimate.

The simulations were conducted using pyEIT [12]. The forward and inverse meshes consisted of 287 and 152 triangular elements respectively, as shown in Fig. 2. 16 electrodes were placed equispaced on the boundary of the surface. We used the "opposite" current pattern with a total of 16 linearly independent current patterns of 12 voltage measurements each. The target was modelled as spanning a single mesh element and randomly moving to an adjacent element at each time step. The baseline conductivity was set at 1 S/m and the conductivity of the target at 10 S/m. For the hyperparameter in (7), we used the value $\lambda = 0.01$.

The position of the target was initialized randomly and moved randomly to an adjacent element of the previous location at each time step. The forward problem was solved independently for each frame. The number of frames used was 500, as it was a sufficient number for the information about the initial position of the target to mostly disappear ($|\lambda_2|^{500} \leq 0.01$, where λ_2 is the eigenvalue of $\mathbf{P}$ with the second-largest absolute value). Zero-mean Gaussian noise was added to the forward voltage measurements. Five different levels of added noise were used: -100 dB, -80 dB, -60 dB, -40 dB, and -20 dB. The added noise level is in relation to the voltage measurements, $\mathbf{v}$. Our true input signal is the difference in voltage measurements between surface with a target and empty surface. Since the voltage differences are much smaller than the absolute voltage values, the dB values do not reflect our true signal-to-noise ratio. The experiment was repeated 100 times for each noise level. The performance of each algorithm was evaluated measuring the mean square error between the true target center and the predicted target center for each setup, averaged over both time and samples. This metric is also used in [16].

The results of the experiment are shown in Fig. 3. It can be seen that our method (HMM) outperforms a simple reconstruction (JAC) and a Kalman filter approach (KF) at all noise levels. The relative performance of the HMM is also consistent across all noise levels. In contrast, simple reconstruction fails at high noise levels and the Kalman filter performs poorly at low noise levels as shown in Fig. 4.

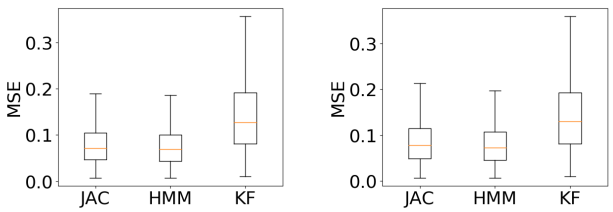

(a) Noise level -100 dB

(b) Noise level -80 dB

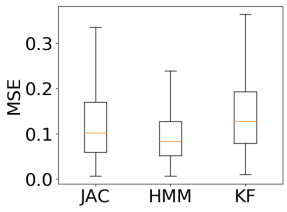

(c) Noise level -60 dB

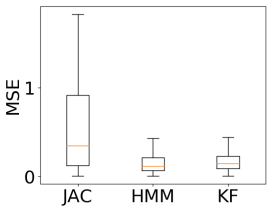

(d) Noise level -40 dB

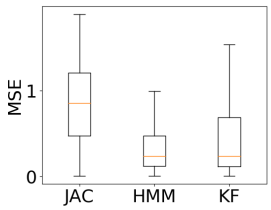

(e) Noise level -20 dB

Fig. 3: Mean square errors (MSE) of predicted target centers for different algorithms and noise levels. Note the different y-axes on the graphs.

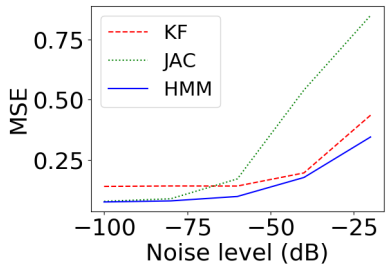

Fig. 4: Noise level versus mean square error.

V. Conclusion

In this paper, we developed a method for tracking a moving target from EIT data and compared that against state-of-the-art temporal EIT methods. Our method outperforms existing methods for temporal EIT.

There are also several fruitful areas for further work. In this paper, we limited our experiments to a single small target with a random walk as the kinematic model of its movement. A natural extension of the method would be to model other kinematic models such as targets moving on constant velocity or acceleration. Further research might also explore combining the studied methods with multitarget tracking [17] to the EIT environment and our method. Another interesting direction for future research is to compare these methods with particle filtering methods [18], where the model parameters could be estimated jointly with tracking.

References

[1] J. Cheng, M. Sundholm, B. Zhou, M. Hirsch, and P. Lukowicz, "Smart-surface: Large scale textile pressure sensors arrays for activity recognition," *Pervasive and Mobile Computing*, vol. 30, pp. 97–112, Aug. 2016.

[2] Y. Zhang, G. Laput, and C. Harrison, "Electrick: Low-Cost Touch Sensing Using Electric Field Tomography," in *Proceedings of the 2017 CHI Conference on Human Factors in Computing Systems*, Denver, Colorado, USA, May 2017, pp. 1–14.

[3] Y. Kato, T. Mukai, T. Hayakawa, and T. Shibata, "Tactile sensor without wire and sensing element in the tactile region based on EIT method," in *SENSORS, 2007 IEEE*. 2007, pp. 792–795, IEEE.

[4] M. Hallaji, A. Seppänen, and M. Pour-Ghaz, "Electrical impedance tomography-based sensing skin for quantitative imaging of damage in concrete," *Smart Materials and Structures*, vol. 23, no. 8, pp. 085001, June 2014.

[5] S. Yoshimoto, Y. Kuroda, and O. Oshiro, "Tomographic Approach for Universal Tactile Imaging With Electromechanically Coupled Conductors," *IEEE Transactions on Industrial Electronics*, vol. 67, no. 1, pp. 627–636, 2020.

[6] O. K. Lee, H. Kang, J. C. Ye, and M. Lim, "A non-iterative method for the electrical impedance tomography based on joint sparse recovery," *Inverse Problems*, vol. 31, no. 7, pp. 075002, 2015.

[7] J. Snyder, Y. Silverman, Y. Bai, and M. A. MacIver, "Underwater object tracking using electrical impedance tomography," in *2012 IEEE/RSJ International Conference on Intelligent Robots and Systems*, Oct. 2012, pp. 520–525.

[8] A. Adler, T. Dai, and W. R. B. Lionheart, "Temporal image reconstruction in electrical impedance tomography," *Physiological Measurement*, vol. 28, no. 7, pp. S1–S11, 2007.

[9] M. Vauhkonen, P. A. Karjalainen, and J. P. Kaipio, "A Kalman filter approach to track fast impedance changes in electrical impedance tomography," *IEEE Transactions on Biomedical Engineering*, vol. 45, no. 4, pp. 486–493, 1998.

[10] K. Y. Kim, B. S. Kim, M. C. Kim, Y. J. Lee, and M. Vauhkonen, "Image reconstruction in time-varying electrical impedance tomography based on the extended Kalman filter," *Measurement Science and Technology*, vol. 12, no. 8, pp. 1032–1039, 2001.

[11] J. L. Mueller and S. Siltanen, *Linear and Nonlinear Inverse Problems with Practical Applications*, Society for Industrial and Applied Mathematics, Philadelphia, PA, USA, 2012.

[12] B. Liu, B. Yang, C. Xu, J. Xia, M. Dai, Z. Ji, F. You, X. Dong, X. Shi, and F. Fu, "pyEIT: A python based framework for Electrical Impedance Tomography," *SoftwareX*, vol. 7, pp. 304–308, 2018.

[13] A. Borsic, B. M. Graham, A. Adler, and W. R. B. Lionheart, "Total Variation Regularization in Electrical Impedance Tomography," Tech. Rep. 92, School Math., Univ. Manchester, Manchester, U.K, 2007.

[14] M. Vauhkonen, D. Vadasz, P. A. Karjalainen, E. Somersalo, and J. P. Kaipio, "Tikhonov regularization and prior information in electrical impedance tomography," *IEEE transactions on medical imaging*, vol. 17, no. 2, pp. 285–293, 1998.

[15] A. Viterbi, "Error bounds for convolutional codes and an asymptotically optimum decoding algorithm," *IEEE Transactions on Information Theory*, vol. 13, no. 2, pp. 260–269, Apr. 1967, Conference Name: IEEE Transactions on Information Theory.

[16] H. Gagnon, B. Grychtol, and A. Adler, "A comparison framework for temporal image reconstructions in electrical impedance tomography," *Physiological measurement*, vol. 36, no. 6, pp. 1093–1107, 2015.

[17] Y. Bar-Shalom and X. R. Li, *Multitarget-Multisensor Tracking: Principles and Techniques*, YBS Publishing, Storrs, CT, USA, 1995.

[18] C. Andrieu, A. Doucet, and R. Holenstein, "Particle Markov chain Monte Carlo methods," *Journal of the Royal Statistical Society: Series B (Statistical Methodology)*, vol. 72, no. 3, pp. 269–342, 2010.